We are IntechOpen,
the world's leading publisher of Open Access books
Built by scientists, for scientists

6,900
Open access books available

186,000
International authors and editors

200M
Downloads

Our authors are among the

154
Countries delivered to

TOP 1%
most cited scientists

12.2%
Contributors from top 500 universities

CLARIVATE ANALYTICS
BOOK CITATION INDEX
INDEXED

WEB OF SCIENCE™

Selection of our books indexed in the Book Citation Index
in Web of Science™ Core Collection (BKCI)

Interested in publishing with us?
Contact book.department@intechopen.com

Numbers displayed above are based on latest data collected.
For more information visit www.intechopen.com

Motion Control of Biped Lateral Stepping Based on Zero Moment Point Feedback for Adaptation to Slopes

Satoshi Ito and Minoru Sasaki
Gifu University
Japan

1. Introduction

Biped locomotion consists of both sagittal and lateral (frontal) plane motions. Although the stability of the locomotion must be ensured in both the planes, their natures are different. In the sagittal plane, the main purpose is to move from one place to another; thus, the stability is dynamic – losing static balance is essential in sagittal plane motion; it produces tumble for travel. In the lateral plane, on the other hand, maintaining an upright posture is crucial. Hence, lateral stability is static, and stabilizing a saddle point in the phase plane of the inverted pendulum motion is the main challenge.

In general, the zero moment point (ZMP) criterion is utilized for biped motion control (Kagami et al., 2002; Mitobe et al., 2001; Nagasaka et al., 1999; Suleiman et al., 2009; Yamaguchi & Takanishi, 1997). Although this method is effective and useful, planned motion using this method is not suitable when the environmental conditions change from those considered during motion planning. The literature offers excellent reports on the modification of planned motion (Hirai et al., 1998; Huang et al., 2000; Kulvanit et al., 2005; Lee et al., 2005; Napoleon & Sampei, 2002; Prahlad et al., 2007; Wollherr & Buss, 2004), or online motion generation (Behnke, 2006; Czarnetzki et al., 2009; Héliot & Espiau, 2008; Kajita & Tani, 1996; Nishiwaki et al., 2002; Sugihara et al., 2002) that solve this problem.

Usually, motion planning based on the ZMP criterion is applied to both the sagittal and lateral planes. The concept of this paper is that motion planning in the lateral plane can be skipped because of the difference in the nature of its stability. In the sagittal plane, motion planning is certainly crucial: one cannot proceed without actively generating both leg swing and torso behaviour, followed by the planned motion. The ZMP method was originally proposed to design such co-ordinated motions. However, in the lateral plane, balance is the primary purpose; generating active motion is a secondary problem. Nonetheless, in the ZMP method, the motion is first planned, and balance is maintained as a result of exact tracking of the planned motion. In our opinion, the process should be reversed for motion in the lateral plane, with balance control coming first and motion emerging as a result of balance control. From this viewpoint, trajectory generation for the lateral plane should be eliminated by setting balance as the control object.
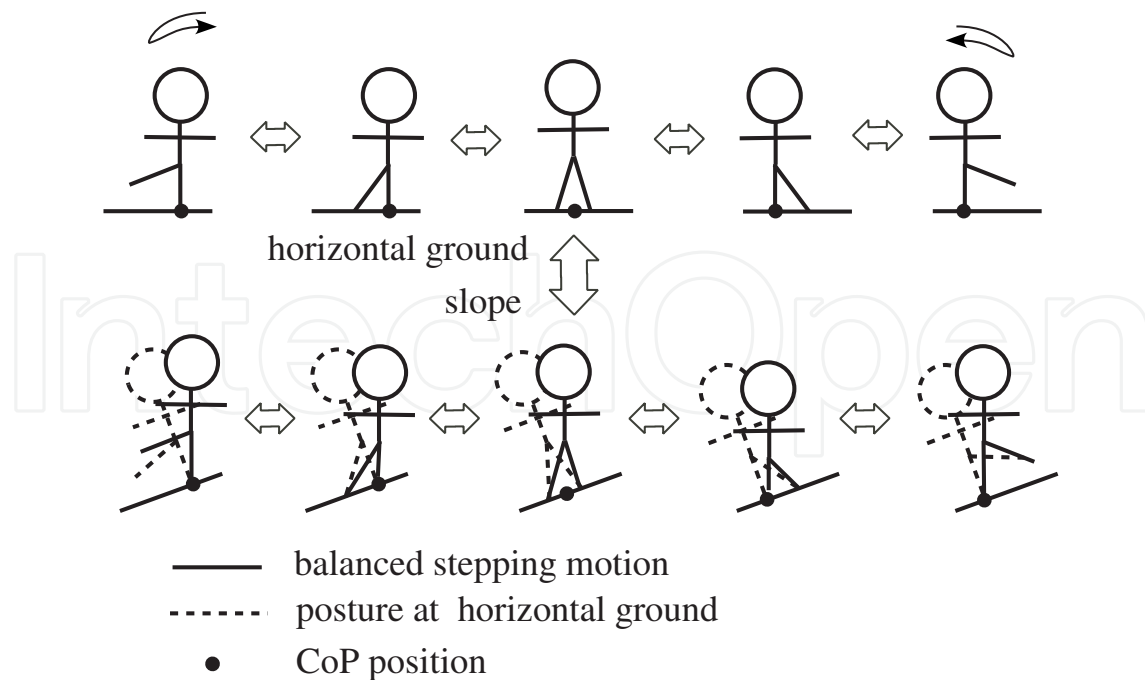
Fig. 1. Lateral stepping motion on different gradients.

To maintain balance without motion planning, we introduce the direct centre of pressure (CoP), i.e. ZMP control (Ito et al., 2003; 2007; 2008) (the CoP is equivalent to the ZMP). Instead of an indirect balancing method, such as tracking the positions of trajectories planned using the ZMP criterion, we select the ZMP directly as the control variable.

Adaptive lateral motion should result without adjusting the controllers or motion pattern generators. This arises from the invariance in the ZMP trajectory in biped lateral motion. Lateral motion on flat and sloped floors is illustrated in Fig. 1. To maintain balance, the motion trajectories of the torso and legs must change adaptively in relation to the angle of the slope. On the other hand, the ZMP trajectory, indicating the time stamp of the load centre, is invariable. Therefore, balance control based on direct ZMP control can naturally produce adaptive motion without re-designing the motion trajectories. In this chapter, we explain a balance control strategy based on direct ZMP feedback and confirm the effectiveness of this method by conducting experiments of improved robot from our previous papers (Ito et al., 2007; 2008).

This chapter is organized as follows: the next section presents the mathematical framework; section 3 describes a control method based on the direct ZMP control; section 4 reports on robot experiments as well as simulation of lateral stepping motion and the section 5 presents our conclusions.

2. Basic Theory of balance control

2.1 Inverted Pendulum model

2.1.1 Assumptions

The CoP is the representative action point of the ground reaction forces and coincides with the ZMP (Goswami, 1999). Because the ZMP contains significant information on balance, the ground reaction forces are also expected to contain the information.
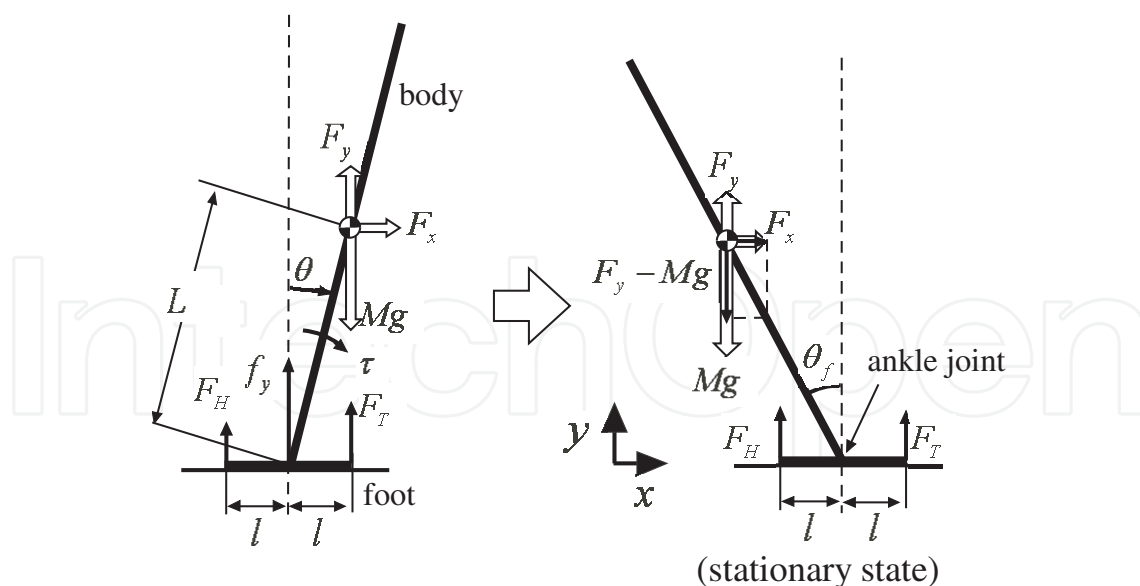
Fig. 2. Inverted pendulum model for biped balance.

From this viewpoint, feedback control of ground reaction forces is introduced for balance control (Ito & Kawasaki, 2005). Because the ankle strategy is dominant for balancing with respect to small disturbances (Horak & Nashner, 1986), the inverted pendulum model illustrated in the left of Fig. 2 is considered with the following assumptions:

- The motion occurs only in the sagittal plane.
- The body (inverted pendulum) and the foot (support) are connected at the ankle joint.
- The foot does not slip on the ground.
- The shape of the foot is symmetrical in the anterior-posterior direction.
- The foot has two ground contact points: the heel and the toe.
- The vertical component of the ground reaction force is measurable.
- The ankle joint is located at the midpoint of the foot with zero height.
- The ankle joint angle and its velocity are detectable.
- An appropriate torque is actively generated at the ankle joint.
- An unknown constant external force is exerted at the centre of gravity (CoG).

The notations are defined as follows: M and m are the mass of the body and foot link, respectively; I is the moment of inertia of the body link around the ankle joint; L is the length between the ankle joint and the CoG of the body link; ℓ is the length from the ankle joint to the toe or the heel; θ is the ankle joint angle; $\dot{\theta}$ is its velocity and τ is the ankle joint torque. F_H and F_T are the vertical components of the ground reaction force at the heel and the toe, respectively. f_y is the vertical component of the internal force between the two links. F_x and F_y are the horizontal and vertical components of constant external force, respectively, and g is the gravitational acceleration.

2.1.2 Control law

The goal of the control is to maintain the postural balance regardless of the constant external forces F_x and F_y. With respect to the stability margin (McGhee & Frank, 1968), F_T and F_H should be kept equal, indicating that the ZMP is held to the centre under the foot. The following control method achieves this.

Theorem 1. *Define an ankle joint torque τ by using adequate feedback gains K_d, K_p, K_f and adequate constant θ_d as*

$$\tau = -K_d\dot{\theta} + K_p(\theta_d - \theta) + K_f \int (F_H - F_T)dt. \tag{1}$$

Then, $\theta = \theta_f$ becomes a locally asymptotically stable posture, and $F_H = F_T$ holds at the stationary state. Here, θ_f is a constant satisfying

$$\sin\theta_f = -\frac{F_x}{A}, \quad \cos\theta_f = \frac{Mg - F_y}{A}. \tag{2}$$

where

$$A = \sqrt{(Mg - F_y)^2 + F_x^2} \tag{3}$$

Proof. The motion equation of the body link is described as

$$\begin{aligned} I\ddot{\theta} &= MLg\sin\theta + F_xL\cos\theta - F_yL\sin\theta + \tau. \\ &= AL\sin(\theta - \theta_f) + \tau \end{aligned} \tag{4}$$

On the other hand, the ground reaction forces, with ankle joint torque, are

$$F_T = -\frac{1}{2\ell}\tau + \frac{1}{2}mg + \frac{1}{2}f_y, \tag{5}$$

$$F_H = \frac{1}{2\ell}\tau + \frac{1}{2}mg + \frac{1}{2}f_y, \tag{6}$$

Here, a new state variable τ_f is defined as

$$\tau_f = \int (F_H - F_T)dt. \tag{7}$$

Then, the control law (1) becomes

$$\tau = -K_d\dot{\theta} + K_p(\theta_d - \theta) + K_f\tau_f. \tag{8}$$

which is regarded as a state feedback whose states are θ, $\dot{\theta}$ and τ_f. In addition, differentiating (7) and then substituting (5) and (6) results in

$$\dot{\tau}_f = \frac{1}{\ell}\tau. \tag{9}$$

An equilibrium point $(\bar{\theta}, \bar{\dot{\theta}}, \bar{\tau}_f)$ of the dynamics in (4) and (9) with control law (8) is obtained by setting the time-derivative term as zero. It is given as

$$(\bar{\theta}, \bar{\dot{\theta}}, \bar{\tau}_f) = (\theta_f, 0, \frac{K_p}{K_f}(\theta_f - \theta_d)). \tag{10}$$
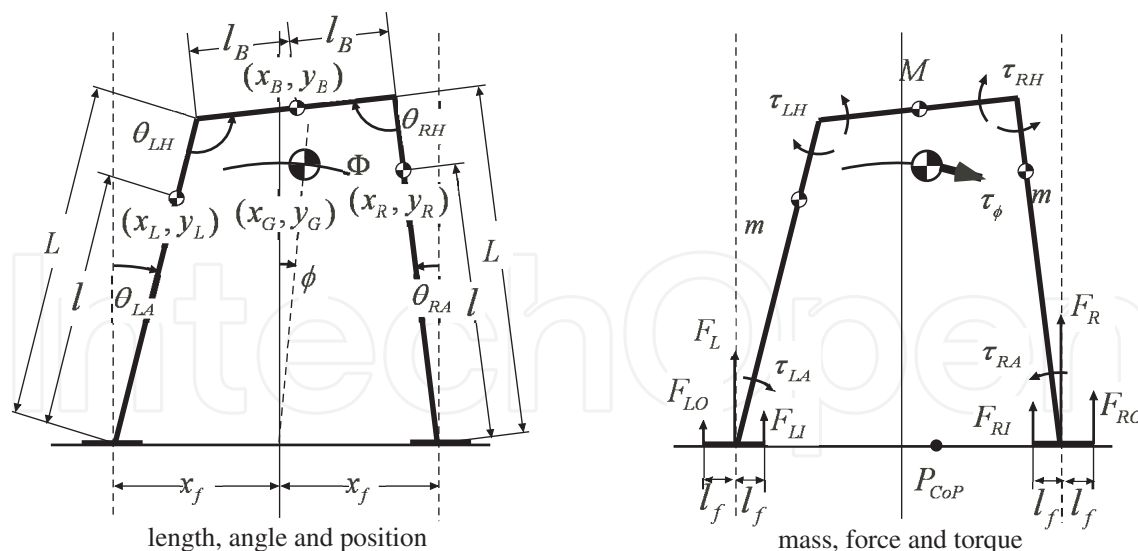
Fig. 3. Lateral sway model for biped balance.

In this state, $\tau = 0$ holds according to (8) and (10), indicating that $F_H = F_T$. The local stability of this equilibrium point is ensured by the controllability of the linearized dynamics around this point. □

2.1.3 Behaviour
The stationary posture from the control law in (1) is illustrated in the right of Fig. 2. This stationary state θ_f depends not on θ_d but the external forces F_x and F_y. It follows that the stationary posture changes adaptively with respect to the environmental conditions expressed as unknown constant external forces. This posture allows the ankle joint torque to be zero in the stationary state, since the moment of the external force is balanced by that of the gravity around the ankle joint. This is an advantage of the control law, in addition to being a model-free property.

2.2 Lateral Sway model
2.2.1 Assumptions
Here, we extend the control law in (1) to active lateral sway with double support. Because the flexion of knee joints in this motion is small, each leg is represented by only one link, without a knee, as shown in Fig. 3. Thus, the following assumptions are introduced:

- The motion is restricted within the lateral plane.
- The lateral motion is approximately represented using a 5-link model consisting of one body, two legs and two feet.
- The foot does not slip on the ground.
- Ankle joints are assumed to be located at the centre of the foot with zero height.
- At the end of both sides, the feet contact the ground.
- The vertical component of the ground reaction forces is measurable.
- The angles and velocities are detectable at the ankle and hip joints.
- Every joint is actively actuated.

• An unknown constant external force is exerted on the CoG of the entire body.

Assume that the feet always maintain contact with the ground. This constraint forces the mechanism to be a closed link constructed by the body and two legs, indicating that the degree of freedom (DoF) of motion is reduced to one.

Here, the following notations are defined: (x_G, y_G) denotes the CoG position in the coordinate frame whose origin is set at the midpoint between two ankle joints, ϕ is a lateral sway angle in this coordinate frame. (x_R, y_R), (x_L, y_L) and (x_B, y_B) are the CoG of the right leg, left leg and body (pelvis), respectively. L is the length of the leg, ℓ is the length from the ground to the CoG of the leg, ℓ_B is the half length of the body, ℓ_f is the length from the ankle joint to the side of the foot and x_f is the distance to the ankle joint from the origin of this coordinate frame. F_{RO}, F_{RI}, F_{LO}, and F_{LI} are the vertical components of ground reaction forces at four contact points, whose subscripts $_{RO}$, $_{RI}$, $_{LI}$ and $_{LO}$ represent the positions of the contact points, indicating the right outside, the right inside, the left inside and the left outside, respectively. $\mathbf{F} = [F_x, F_y]^T$ is the external force that is assumed to be constant. $\Theta = [\theta_{RA}, \theta_{RH}, \theta_{LH}, \theta_{LA}]^T$ is a joint angle vector whose elements are the joint angles of the right ankle, right hip, left hip and left ankle, respectively, and $\mathbf{T} = [\tau_{RA}, \tau_{RH}, \tau_{LH}, \tau_{LA}]^T$ is a joint torque vector whose elements are the torque at each joint. τ_ϕ is a generalized force defined in the coordinate frame on the CoG orbit Φ, and P_{ZMP} is the position of the ZMP.

2.2.2 Control law

Under these assumptions, P_{ZMP} is calculated from the magnitude of the ground reaction forces at the four contact points as follows:

$$P_{ZMP} = \frac{F_{RO}}{F_{all}}(x_f + \ell_f) + \frac{F_{RI}}{F_{all}}(x_f - \ell_f) - \frac{F_{LI}}{F_{all}}(x_f - \ell_f) - \frac{F_{LO}}{F_{all}}(x_f + \ell_f), \quad (11)$$

where

$$F_{all} = F_{RO} + F_{RI} + F_{LI} + F_{LO}. \quad (12)$$

The purpose is to control the position of the ZMP at its reference position P_d in the lateral sway model, as shown in Fig. 1. Here, P_d is appropriately planned in advance and may be constant or, alternatively, switched. This is achieved using ZMP feedback obtained by extending theorem 1.

Theorem 2. *Define a generalized force τ_ϕ based on P_{ZMP} as*

$$\tau_\phi = -K_d\dot{\phi} + K_p(\phi_d - \phi) + K_f \int (P_d - P_{ZMP})dt, \quad (13)$$

and assign each joint torque $\mathbf{T}$ so that the following equation holds

$$\tau_\phi = \mathbf{J}^T(\Theta)\mathbf{T}. \quad (14)$$

Here, ϕ_d is a constant, and $\mathbf{J}(\Theta)$ is a Jacobian matrix that relates the deviation of Θ to that of ϕ

$$\Delta\Theta = \mathbf{J}(\Theta)\Delta\phi. \quad (15)$$

Then, P_{ZMP} converges to P_d if it starts in the neighbourhood of P_d.

Proof. Because there is only one DoF of the lateral sway model, the sway angle ϕ uniquely determines each joint angle Θ in the range $0 < \theta_{RH} < \pi, 0 < \theta_{LH} < \pi$. Here, this relationship is described as $\Theta = \Theta(\phi)$. Then, the equation of motion with respect to ϕ is obtained as

$$M(\Theta)\ddot{\phi} + C(\Theta, \dot{\Theta}) + G(\Theta, g, \mathbf{F}) = \tau_\phi. \tag{16}$$

On the other hand, the relationship between P_{ZMP} and τ_ϕ is given as

$$P_{ZMP} = P(\Theta)\tau_\phi + Q(\Theta, \dot{\Theta}) + R(\Theta, g, \mathbf{F}). \tag{17}$$

Here, $M(\Theta) > 0$ is an inertia term, $C(\Theta, \dot{\Theta})$ and $Q(\Theta, \dot{\Theta})$ become the second order terms of the element of $\dot{\Theta}$, G and R contain both the gravity term and external force $\mathbf{F}$. See Appendix 7.3 for the derivation of (16) and (17). Then, a new variable τ_f is introduced:

$$\tau_f = \int (P_{ZMP} - P_d)dt. \tag{18}$$

The differentiation of τ_f provides the relationship

$$\dot{\tau}_f = P_{ZMP} - P_d. \tag{19}$$

And, using (17), it becomes

$$\dot{\tau}_f = P(\Theta)\tau_\phi + Q(\Theta, \dot{\Theta}) + R(\Theta, g, \mathbf{F}) - P_d. \tag{20}$$

In addition, the control law in (13) is described using τ_f

$$\tau_\phi = -K_d\dot{\phi} + K_p(\phi_d - \phi) + K_f\tau_f. \tag{21}$$

Let $[\phi, \dot{\phi}, \tau_f]^T$ be state variables of the dynamics of (16) and (20) with the control law in (21). At the equilibrium point, the derivative terms are forced to zero, indicating that $\dot{\tau}_f = 0$ in (19); thus, $P_{ZMP} = P_d$. To test the stability of the equilibrium point, (16) and (20) are linearized around it.

$$\dot{\xi} = \begin{bmatrix} 0 & 1 & 0 \\ -\bar{G}_\theta \bar{J}/\bar{M} & 0 & 0 \\ (\bar{R}_\theta + \bar{P}_\theta \bar{\tau}_\phi)\bar{J} & 0 & 0 \end{bmatrix} \xi + \begin{bmatrix} 0 \\ 1/\bar{M} \\ \bar{P} \end{bmatrix} \Delta\tau_\phi \tag{22}$$

Here, $\xi = [\Delta\phi, \Delta\dot{\phi}, \Delta\tau_f]^T$ is a deviation from the equilibrium point, $\bar{M} = M(\bar{\Theta})$, $\bar{\Theta} = \Theta(\bar{\phi})$, $\bar{J} = J(\bar{\Theta})$, $\bar{P} = P(\bar{\Theta})$, $\bar{G}_\theta = \dfrac{\partial G(\bar{\Theta})}{\partial \Theta}$, $\bar{R}_\theta = \dfrac{\partial R(\bar{\Theta})}{\partial \Theta}$, $\bar{P}_\theta = \dfrac{\partial P(\bar{\Theta})}{\partial \Theta}$, and $\Delta\tau_\phi$ is a deviation from the input at the equilibrium $\bar{\tau}_\phi = K_p(\phi_d - \bar{\phi}) + K_f\bar{\tau}_f$. The controllability matrix M_c of this linear system becomes

$$M_c = \begin{bmatrix} 0 & 1/\bar{M} & 0 \\ 1/\bar{M} & 0 & -\bar{G}_\theta\bar{J}/\bar{M}^2 \\ \bar{P} & 0 & (\bar{R}_\theta + \bar{P}_\theta\bar{\tau}_\phi)\bar{J}/\bar{M} \end{bmatrix}, \tag{23}$$

whose determinant is calculated as

$$|M_c| = -\frac{1}{\bar{M}^3}(\bar{P}\bar{G}_\theta + \bar{R}_\theta + \bar{P}_\theta\bar{G})\bar{J} = -\frac{1}{\bar{M}^3}\left.\frac{\partial}{\partial\phi}(PG + R)\right|_{\phi=\bar{\phi}}. \tag{24}$$

Here, the relationship $\bar{\tau}_\phi = \bar{G} = G(\bar{\Theta})$ from (16) and $\bar{J} = \frac{\partial \Theta}{\partial \phi}$ were applied. To verify $|M_c| \neq 0$, the deviation of the ZMP position is considered. Substituting (16) into τ_ϕ of (17) and linearizing (17) around the equilibrium point results in

$$\Delta P_{ZMP} = PM\Delta\ddot{\phi} + \frac{\partial}{\partial \phi}(PG + R)\Big|_{\phi = \bar{\phi}} \Delta\phi. \tag{25}$$

This equation implies that the ZMP deviation depends on both the inertial force (the first term) and the gravitational effect (the second term), which varies with the posture, i.e. the CoG position. This is consistent with the definition of the ZMP – it is determined by the inertial and gravitational forces. Now, assume $|M_c| = 0$. Then, $\frac{\partial}{\partial \phi}(PG + R)\Big|_{\phi = \bar{\phi}} = 0$ from (24). This produces the conclusion, based on (25), that the ZMP position does not change regardless of the CoG deviation. This contradicts the definition of ZMP; thus, $|M_c| \neq 0$ is ensured. Accordingly, the controllability matrix M_c should be full rank and the linear system is controllable – the equilibrium point can be stabilized by adequate K_d, K_p and K_f in (13). Finally, note that we can find joint torque $\mathbf{T}$ to satisfy the relationship in (14). ☐

2.2.3 Behaviour
The behaviour of the lateral sway model under control laws (13) - (15) is expected to be similar to that of the inverted pendulum model using control law (1) discussed in the section 2.1.3, i.e., in the stationary state:

- The ZMP is controlled to its reference position P_d.

- The posture changes with the external force.

- The generalized force τ_ϕ becomes zero due to the balance between the gravitational and external forces.

Thus, this control law is a natural extension of control law (1) when there are multiple contact points and active joints.

3. Control of in-place stepping

3.1 Strategy
Here, we focus on in-place stepping motion to achieve it without generating reference trajectories of joint angles, as expected in section 1. The stepping motion is divided into single- and double-support phases. The control law is defined separately in these two phases, and then, two theorems from the previous section are applied, since this task basically involves the stabilization of the inverted pendulum with respect to external forces caused by ground gradients. However, some extensions are needed: definition of the switching conditions between the two control laws and the time-dependent reference for the ZMP position. The local stability of the control laws will ensure tracking of the ZMP position to the time-dependent reference.

3.2 Control
3.2.1 Single-support phase
On a slope, adaptive behaviour is observed – the body tilts around the ankle joint of the supporting leg, as shown in the bottom of Fig. 1. Thus, the ankle joint plays a significant role,
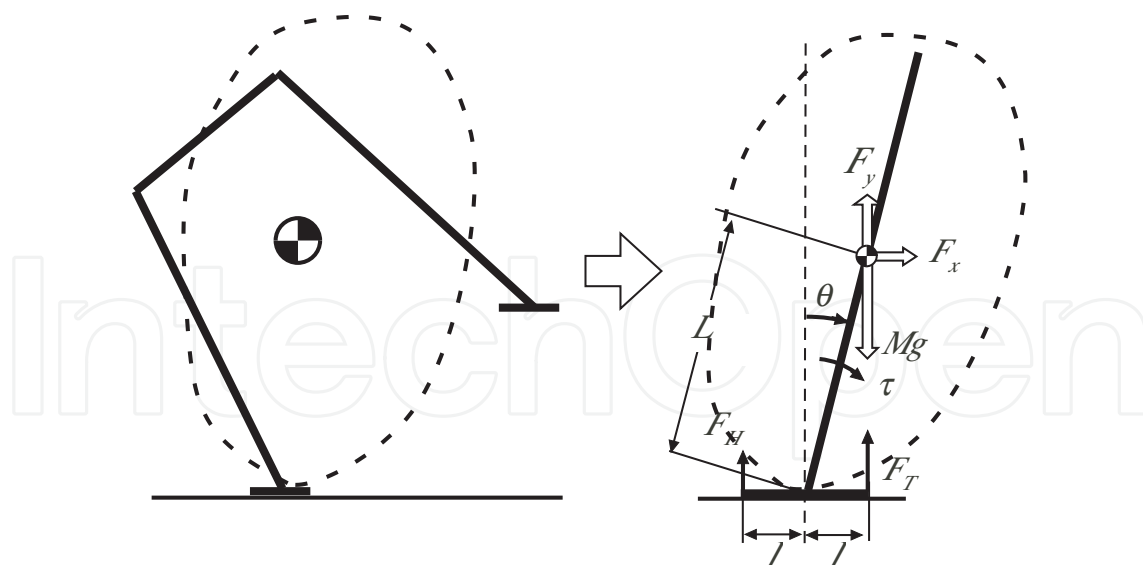
Fig. 4. Single-support phase approximation by using the inverted pendulumn model.

and the dynamics of the single-support phase can be approximated by an inverted pendulum
with a foot support, as shown in Fig. 4. Under this approximation, theorem 1 is applicable by
regarding the effect of the slope as well as the swing leg dynamics as unknown external forces
F_x and F_y. The flow of the balance control is summarized as

1. Detect the angle and its velocity at the ankle joint of the support leg.

2. Detect the ground reaction forces at both ends of the supporting foot.

3. Calculate the ankle joint torque according to (1).

4. Output the ankle joint torque with its actuator.

The trajectory tracking control should be introduced to lift the swing leg.

3.2.2 Switching from single- to double-support phase

Control law (1) is expected to compensate for disturbances caused by the torso and swing leg
when stepping. If the torso and swing leg motions are adequately controlled, the posture of
the initial state of the single-support phase will be recovered. Thus, the switch condition of
the control law is set as the recovery of the initial posture.

3.2.3 Double-support phase

To change to the other support leg, the ZMP position must shift from under the current
supporting leg to the other. Control laws (13) - (15) are expected to make the ZMP track
such a reference position P_d. Following is the control flow:

1. Detect the angle and its velocity at the ankle and hip joints.

2. Detect the ground reaction forces at both ends of the feet.

3. Calculate the lateral sway angle ϕ by following the next relationship (Appendix 7.1):

$$\phi = \frac{\theta_{LA} - \theta_{RA}}{2}.$$ (26)

4. Calculate P_{ZMP} by using (11).

5. Compute the generalized force τ_ϕ according to (13).

6. Distribute the generalized force τ_ϕ to each joint torque $\boldsymbol{\tau}$ so as to satisfy (14). Namely,

$$\mathbf{T} = (\mathbf{J}^T(\Theta))^* \tau_\phi + (I - \mathbf{J}^T(\Theta)(\mathbf{J}^T(\Theta))^*)\mathbf{p}. \tag{27}$$

Here, $*$ denotes the generalized inverse matrix, and $\mathbf{p}$ is an arbitrary 4-dimensional vector. See Appendix 7.2 for the calculation of $\mathbf{J}(\Theta)$.

7. Output the joint torque by using the actuators.

3.2.4 Switching from double- to single-support phase

According to control law (13), the ZMP position is shifted to the side of the next supporting leg by following P_d. The control law is switched when the ZMP position reaches an area under the next supporting foot.

4. Robot experiment

4.1 Object

In the previous section, we proposed a control method for lateral stepping that does not require motion planning, i.e. the reference trajectory generation of joint angles. This direct ZMP control is expected to allow a robot to naturally change their motion according to the slope. The objective of this experiment is to confirm this effect by using a robot with reduced DoF. The details of the robot are described in section 4.3.

4.2 Simulation

Prior to the experiments, the control method is simulated under the influence of the constant external force, as expressed by

$$F_x = -Mg \sin \alpha \tag{28}$$

$$F_y = -Mg(1 - \cos \alpha). \tag{29}$$

This is equivalent to the gravitational effect on a slope with angle α. The cases where $\alpha = 0$ [rad] (no external force) and $\alpha = 0.2$ [rad] are examined. The parameters are $M = 2.5$ [kg], $m = 1.25$ [kg], $m_f = 0$ [kg], $L = 0.20$ [m], $\ell = 0.1$ [m], $\ell_B = 0.07$ [m], $\ell_f = 0.02$ [m]. The feedback gains of (1) are set to $K_d = 30$, $K_p = 500$ and $K_f = 1$, while those of (13) are $K_d = 5$, $K_p = 10$ and $K_f = 100$. To the hip joint in the single-support phase, the conventional PD control with non-linear compensation is applied with a reference trajectory that lifts up the swing leg – the feedback gains are $K_d = 100$ and $K_p = 500$.

The graphs in Fig. 5(a) and (b) the ZMP position over time. Regardless of the external forces, similar ZMP profiles are obtained, implying that the body weight shifts as expected in both cases. The time-based plot of the horizontal CoG position is depicted in Fig. 5(c): when the external force is exerted, the stepping motion is performed with the posture tilted against it.

4.3 Equipment

Experiments were performed using a biped robot with four DoFs: two in the hip joints, two in the ankle joints and no DoF other than that in the lateral plane. This is an improved version of that in our previous paper (Ito et al., 2007; 2008). The robot is 35 [cm] high and weighs 2.4 [kg]. The sole of the foot is 8.6 [cm] long and the horizontal distance between the right and
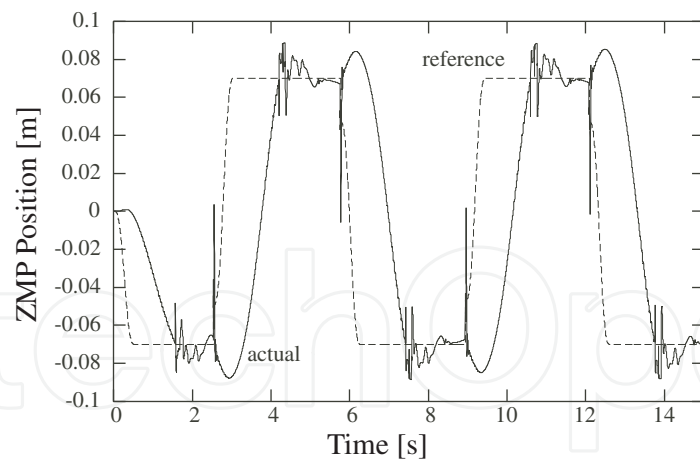
(a) Reference and actual trajectory of ZMP for $\alpha = 0$
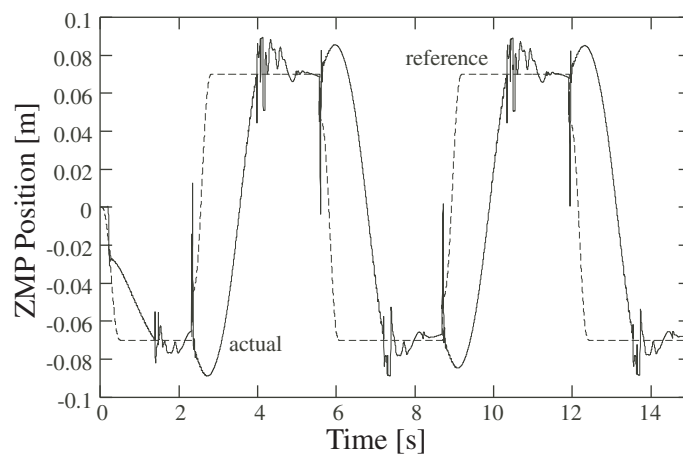
(b) Reference and actual trajectory of ZMP for $\alpha = 0.20$
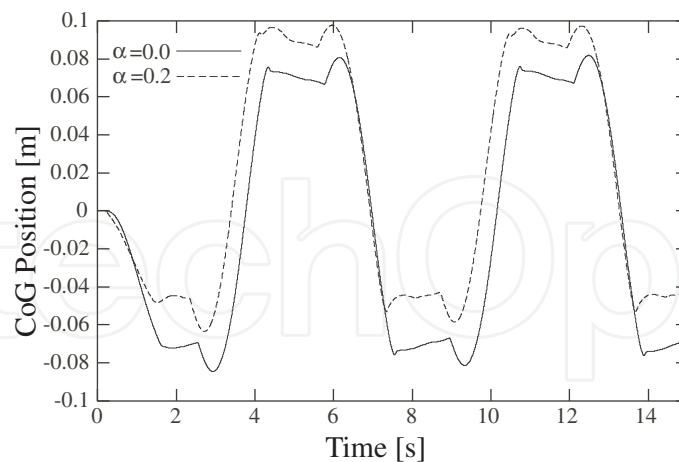

(c) Horizontal position of CoG.

Fig. 5. Simulation results.

left ankles is 13.4 [cm]. Four motors are installed: two drive hip joints, while the others drive ankle joints. A rotary encoder installed in each motor provides information on the joint angles of the robot. Furthermore, three load cells are attached to each sole to provide ZMP detection.
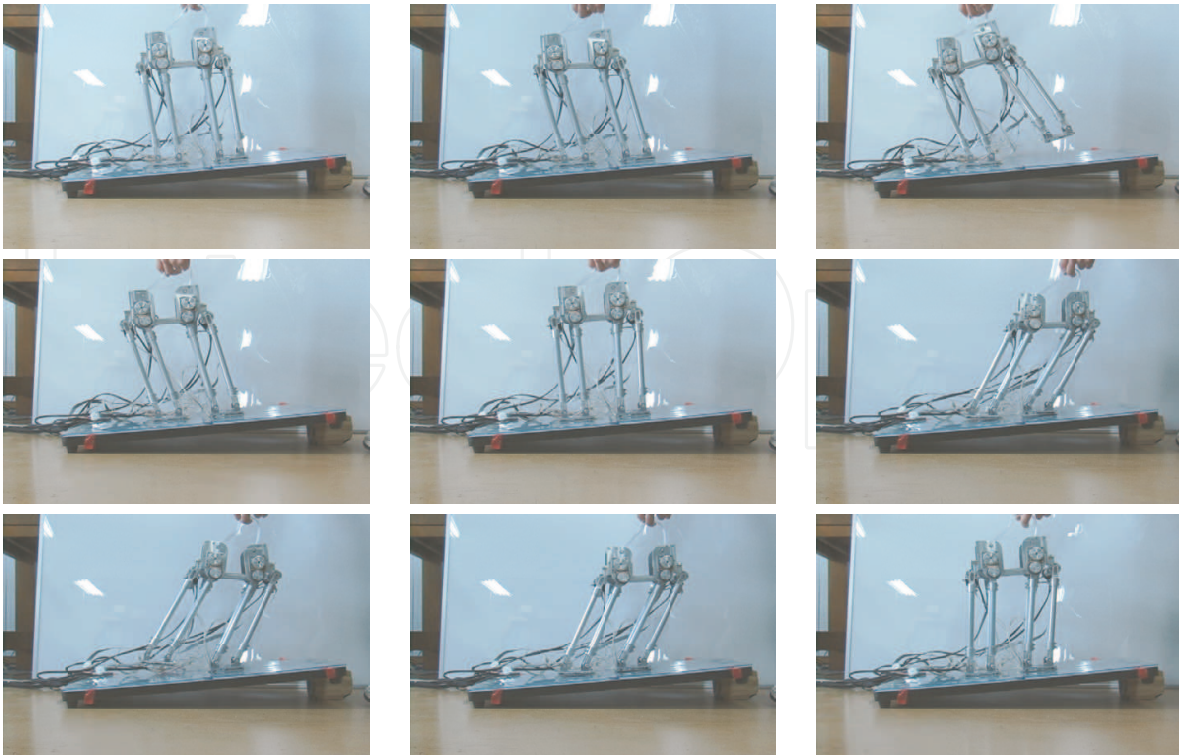
Fig. 6. Snapshots of biped robot experiments on a sloped surface.

The robot controller, operated by ART-LINUX, acquires the sensory information via a pulse counter and A/D converter. It calculates the torque that should be applied at each joint and sends them to the motor driver via a D/A converter. In the experiment, the controller operates at 1 [ms].

4.4 Methods

In the single-support phase, the control law (1) is applied for the ankle joint of the support leg with feedback gains of $K_d = 0.001$, $K_p = 0.005$ and $K_f = 0.0018$. Note that the unit of the angle is set to degrees to allow a simple check of the robot motion in the experiment; thus, the gains are given in the degree unit system. θ in (1) is approximated by the CoG sway angle ϕ, and ϕ at the start of each single-support phase is set to θ_d in (1) so that the ankle joint torque initially becomes zero. The other joint angles are controlled by the PD control. Its reference trajectories are set as follows. The hip joint of the swing leg is held in its neutral position, whereas that of the support leg is extended 30 [deg] from its neutral position in 8 [s], and then, returned to the neutral position again in 8 [s], which is represented by the fifth-order polynomial equation of the time. The ankle joint of the swing leg is controlled so that its sole becomes parallel to the ground at the end of the single-support phase. The control mode is switched when the hip joint angle reaches a neutral position. The feedback gains of the PD control are $K_d = 0.0009$ and $K_p = 0.009$. They are the same for the three joints.

The double-support phase uses control laws (13)-(15). The feedback gains are set to $K_d = 0.001$, $K_p = 0.002$ and $K_f = 0.07$. P_d is set using the fifth-order polynomial equation, to move 18 [cm], i.e. from 8 [cm] (the side of the previous support leg) to 10 [cm] on the reverse side, in 15[s]. To promote ZMP movement, the distance of the ZMP shift is set slightly larger than
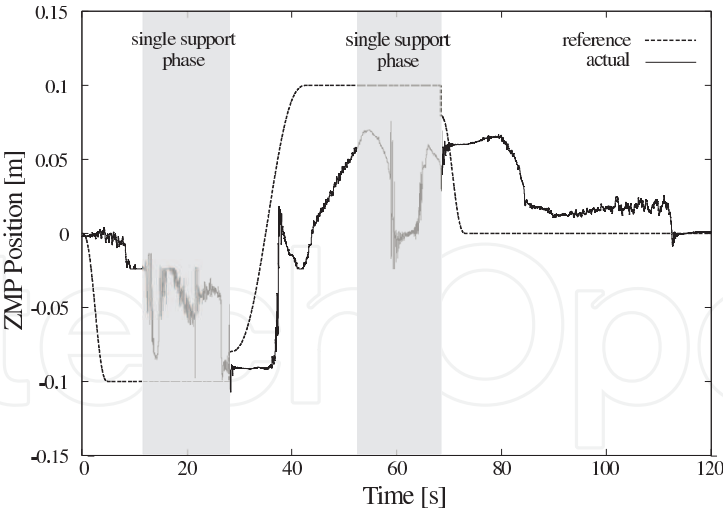
(a) Reference and actual trajectory of ZMP on flat floor.
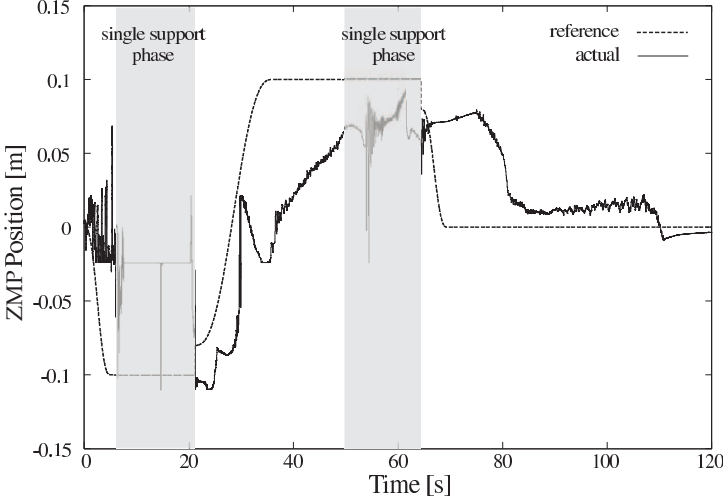
(b) Reference and actual trajectory of ZMP on slope.
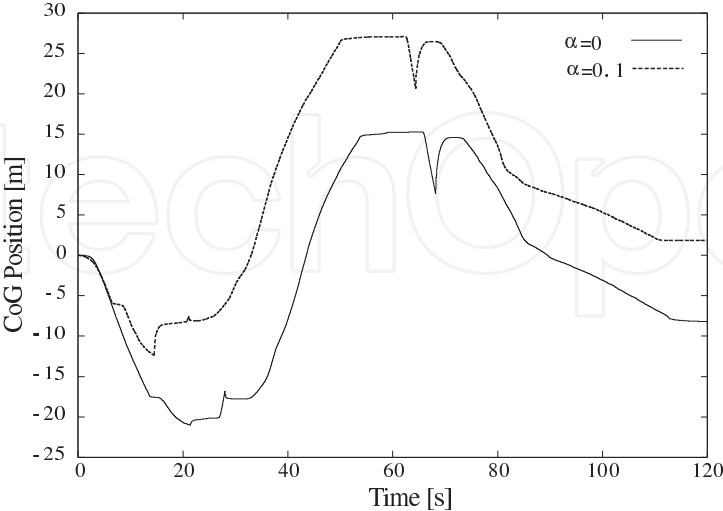
(c) Horizontal position of CoG.

Fig. 7. Experimental results.

the natural width between the two ankle joints (x_f=6.7[cm]). The control mode is switched on the basis of the ZMP position. This threshold is set 7 [cm]. Experiments are executed on both flat ground and an 8 [deg] slope.

4.5 Results and remarks

Snapshots of the robot motion on the slope are shown in Fig. 6. To evaluate the behaviour for both the conditions, time-based plots of the ZMP position in the double-support phase are shown in Fig. 7: (a) is on the flat ground and (b) is on the slope. The ZMP profiles are quite similar, implying that the stepping motion can be achieved regardless of the slope angle. The time based plot of the horizontal CoG position is shown in Fig. 7(c). The profile of the slope condition is shifted up from that on flat ground, indicating that lateral motion is achieved by tilting the entire body adaptively against the slope, as shown in Fig. 1. The slow motion of the robot requires improvement. Correcting mechanical problems, such as backlash at the joints, will improve the motion speed somewhat.

5. Conclusions

The generation of the joint or CoG reference trajectories is a complicated task in biped robot control. By restricting the task to balance control in the lateral plane motion, a control method without the need for generating reference trajectories was proposed. This control method is essentially a feedback control of the ZMP position that makes the most use of the information on the ground reaction forces. Thus, the reference trajectories of both joints and the CoG of the body, which are usually affected by environmental conditions such as the slope, are unnecessary, although those of the ZMP position are required. This approach provides natural adaptive changes in the lateral motion. Applying it to the control of a biped robot, whose DoF of motion were restricted within the lateral plane, experimentally confirmed its effectiveness. Improving the speed of the robot's movements and applying this technique to 3D biped locomotion are considered for future work.

6. Acknowledgement

7. Appendex

7.1 Definition of ϕ

The lateral sway angle ϕ is calculated as

$$\phi = \arctan \frac{x_G}{y_G}. \tag{30}$$

Here, x_G and y_G are the horizontal and vertical positions of the CoG of the lateral sway model, respectively, and are described as

$$x_G = 2\rho \cos \frac{\theta_{RA} + \theta_{LA}}{2} \sin \frac{\theta_{LA} - \theta_{RA}}{2} \tag{31}$$

$$y_G = 2\rho \cos \frac{\theta_{RA} + \theta_{LA}}{2} \cos \frac{\theta_{LA} - \theta_{RA}}{2}, \tag{32}$$

where

$$\rho = \frac{2m\ell + ML}{2(2m + M)}. \tag{33}$$

Using this relationship, we obtain

$$\frac{x_G}{y_G} = \tan \frac{\theta_{LA} - \theta_{RA}}{2}. \tag{34}$$

According to the definition of the generalized coordinates (30), ϕ is expressed by (26), i.e.,

$$\phi = J_{\phi 1}\Theta = J_{\phi 2}X, \tag{35}$$

where

$$J_{\phi 1} = \begin{bmatrix} -\frac{1}{2} & 0 & 0 & \frac{1}{2} \end{bmatrix} \tag{36}$$

$$J_{\phi 2} = \begin{bmatrix} 0 & 0 & 0 & 0 & 0 & \frac{1}{2} & 0 & 0 & -\frac{1}{2} \end{bmatrix}. \tag{37}$$

The definition of X will be seen later in (47).

7.2 Calculation of the Jacobian matrix

The Jacobian matrix $\mathbf{J}(\Theta)$, which maps $\dot{\phi}$ to $\dot{\Theta}$, is calculated as follows. From (26), we get

$$\dot{\phi} = \frac{\dot{\theta}_{LA} - \dot{\theta}_{RA}}{2}. \tag{38}$$

On the other hand, a kinematic relationship among the joint angles is given as

$$-\theta_{RA} + \theta_{RH} + \theta_{LH} - \theta_{LA} = \pi. \tag{39}$$

Differentiating it, we obtain

$$-\dot{\theta}_{RA} + \dot{\theta}_{RH} + \dot{\theta}_{LH} - \dot{\theta}_{LA} = 0. \tag{40}$$

In addition, the position of the left hip joint (x_{RH}, y_{RH}) can be described in two ways:

$$\begin{bmatrix} x_{RH} \\ y_{RH} \end{bmatrix} = \begin{bmatrix} -x_f + L\sin\theta_{RA} \\ L\cos\theta_{RA} \end{bmatrix} = \begin{bmatrix} x_f - L\sin\theta_{LA} - 2\ell_B\sin(\theta_{LH} - \theta_{LA}) \\ L\cos\theta_{LA} - 2\ell_B\cos(\theta_{LH} - \theta_{LA}) \end{bmatrix}. \tag{41}$$

Differentiating them, the following equations hold.

$$\begin{bmatrix} -L\dot{\theta}_{LA}\cos\theta_{LA} - 2\ell_B(\dot{\theta}_{LH} - \dot{\theta}_{LA})\cos(\theta_{LH} - \theta_{LA}) \\ -L\dot{\theta}_{LA}\sin\theta_{LA} + 2\ell_B(\dot{\theta}_{LH} - \dot{\theta}_{LA})\sin(\theta_{LH} - \theta_{LA}) \end{bmatrix} = \begin{bmatrix} L\dot{\theta}_{RA}\cos\theta_{RA} \\ -L\dot{\theta}_{RA}\sin\theta_{RA} \end{bmatrix}. \tag{42}$$

Solve the three equations (38), (40) and (42) as four variables $\dot{\Theta} = [\dot{\theta}_{RA}, \dot{\theta}_{RH}, \dot{\theta}_{LH}, \dot{\theta}_{LA}]^T$ and the relationship between $\dot{\Theta}$ and $\dot{\phi}$ is represented by

$$\dot{\Theta} = \frac{2}{J_1 + J_3} \begin{bmatrix} -J_1 \\ -J_1 + J_2 \\ J_3 - J_2 \\ J_3 \end{bmatrix} \dot{\phi} = \mathbf{J}(\Theta)\dot{\phi} \tag{43}$$
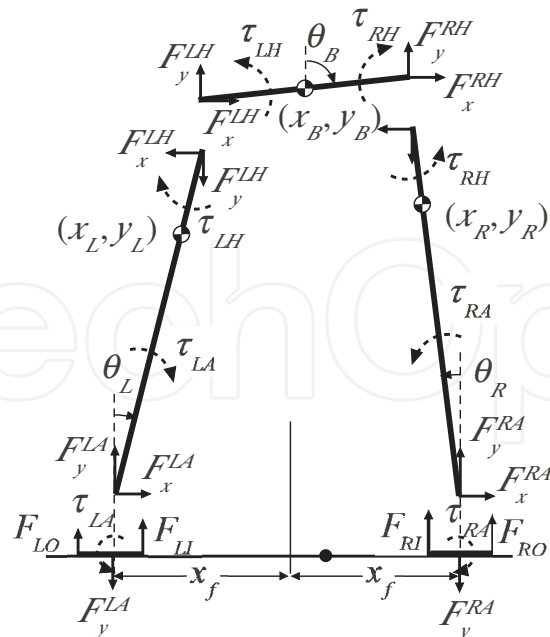
Fig. 8. Notation for the derivation of motion equation.

$$J_1 = 2\ell_B \sin\theta_{LH} \tag{44}$$

$$J_2 = L \sin(\theta_{LH} + \theta_{RH}) \tag{45}$$

$$J_3 = 2\ell_B \sin\theta_{RH}. \tag{46}$$

7.3 Motion equations

We define the vectors X and F as follows:

$$X = [\; x_B \quad y_B \quad \theta_B \quad x_L \quad y_L \quad \theta_L \quad x_R \quad y_R \quad \theta_R \;]^T \tag{47}$$

$$F = [\; F_x^{LH} \quad F_y^{LH} \quad F_x^{RH} \quad F_y^{RH} \quad F_x^{LA} \quad F_y^{LA} \quad F_x^{RA} \quad F_y^{RA} \;]^T. \tag{48}$$

The mechanical constraint is described as

$$C_C(X) = 0, \tag{49}$$

where

$$C_C(X) = \begin{bmatrix} x_B - \ell_B \sin\theta_B - x_L - \ell_s \sin\theta_L \\ y_B - \ell_B \cos\theta_B - y_L - \ell_s \cos\theta_L \\ x_B + \ell_B \sin\theta_B - x_R + \ell_s \sin\theta_R \\ y_B + \ell_B \cos\theta_B - y_R - \ell_s \cos\theta_R \\ x_L - \ell \sin\theta_L \\ y_L - \ell \cos\theta_L \\ x_R + \ell \sin\theta_R \\ y_R - \ell \cos\theta_R \end{bmatrix} \tag{50}$$

$$\ell_s = L - \ell. \tag{51}$$

Refer to Fig. 8 for the notations. The motion equation is expressed as

$$M\ddot{X} = J_X^T F + G_0 + J_\theta^T \mathbf{T}. \tag{52}$$

Here,

$$M = diag[M_B, M_B, I_B, M_L, M_L, I_L, M_L, M_L, I_L] \tag{53}$$

$$J_X = \frac{\partial C_C(\mathbf{X})}{\partial \mathbf{X}} \tag{54}$$

$$G_0 = G_G + J_e^T F_e \tag{55}$$

$$G_G = \begin{bmatrix} 0 & -M_B g & 0 & 0 & -M_L g & 0 & 0 & -M_L g & 0 \end{bmatrix}^T \tag{56}$$

$$J_\theta = \begin{bmatrix} 0 & 0 & 0 & 0 & 0 & 0 & 0 & 0 & 1 \\ 0 & 0 & 1 & 0 & 0 & 0 & 0 & 0 & 1 \\ 0 & 0 & -1 & 0 & 0 & 1 & 0 & 0 & 0 \\ 0 & 0 & 0 & 0 & 0 & 1 & 0 & 0 & 0 \end{bmatrix} \tag{57}$$

$$J_e = \begin{bmatrix} 0 & 0 & 0 & 0 & 0 & \rho \cos\theta_L & 0 & 0 & -\rho \cos\theta_R \\ 0 & 0 & 0 & 0 & 0 & -\rho \sin\theta_L & 0 & 0 & -\rho \sin\theta_R \end{bmatrix} \tag{58}$$

$$F_e = \begin{bmatrix} F_x & F_y \end{bmatrix}^T. \tag{59}$$

Differentiating (49) two times, we obtain

$$J_X \ddot{X} + C_0 = 0, \tag{60}$$

where

$$C_0 = \dot{J}_X \cdot \dot{X}. \tag{61}$$

Combining (52) with (60), we can get

$$\begin{bmatrix} M & -J_X^T \\ -J_X & 0 \end{bmatrix} \begin{bmatrix} \ddot{X} \\ F \end{bmatrix} = \begin{bmatrix} G_0 + J_\theta^T \tau \\ C_0 \end{bmatrix}. \tag{62}$$

The matrix of the left hand side has an inverse matrix since M has it. This inverse matrix is put to

$$\begin{bmatrix} M & -J_X^T \\ -J_X & 0 \end{bmatrix}^{-1} = \begin{bmatrix} N_0 & N_1^T \\ N_1 & N_2 \end{bmatrix}. \tag{63}$$

Then, (62) can be solved for $\ddot{X}$ and F.

$$\begin{bmatrix} \ddot{X} \\ F \end{bmatrix} = \begin{bmatrix} N_0 & N_1^T \\ N_1 & N_2 \end{bmatrix} \begin{bmatrix} G_0 + J_\theta^T \tau \\ C_0 \end{bmatrix}. \tag{64}$$

From (35),

$$\ddot{\phi} = J_{\phi 2} \ddot{X} = J_{\phi 2}(N_0(G_0 + J_\theta^T J_{\phi 1}^T \tau_\phi) + N_1^T C_0). \tag{65}$$

The dynamics of ϕ is expressed by (16), where

$$M(\Theta) = (J_{\phi 2} N_0 J_{\phi 2}^T)^{-1} \tag{66}$$

$$C(\Theta, \dot{\Theta}) = (J_{\phi 2} N_0 J_{\phi 2}^T)^{-1} J_{\phi 2} N_1^T C_0 \tag{67}$$

$$G(\Theta, g, \mathbf{F}) = (J_{\phi2}N_0 J_{\phi2}^T)^{-1} J_{\phi2} N_0 \mathbf{G}_0. \tag{68}$$

Note that $J_{\phi1}J_\theta = J_{\phi2}$ and $\mathbf{X}$ is uniquely written by Θ, i.e., $\mathbf{X} = \mathbf{X}(\Theta)$.
On the other hand, the ground reaction forces are expressed as

$$F_{LO} = \frac{1}{2}F_y^{LA} + \frac{1}{\ell_f}\tau_{LA} \tag{69}$$

$$F_{LI} = \frac{1}{2}F_y^{LA} - \frac{1}{\ell_f}\tau_{LA} \tag{70}$$

$$F_{RO} = \frac{1}{2}F_y^{RA} + \frac{1}{\ell_f}\tau_{RA} \tag{71}$$

$$F_{RI} = \frac{1}{2}F_y^{RA} - \frac{1}{\ell_f}\tau_{RA}. \tag{72}$$

Assume that F_{all} is constant because it corresponds to the total weight. Then, (11) is rewritten as

$$P_{ZMP} = J_{Z1}^T \mathbf{F} + J_{Z2}^T \boldsymbol{\tau} \tag{73}$$

$$J_{Z1} = \begin{bmatrix} 0 & 0 & 0 & 0 & 0 & -x_f/F_{all} & 0 & x_f/F_{all} \end{bmatrix}^T \tag{74}$$

$$J_{Z2} = \begin{bmatrix} 2/F_{all} & 0 & 0 & -2/F_{all} \end{bmatrix}^T. \tag{75}$$

From (64), $\mathbf{F}$ is expressed as

$$\mathbf{F} = N_1(\mathbf{G}_0 + J_\theta^T \boldsymbol{\tau}) + N_2 \mathbf{C}_0. \tag{76}$$

Substituting this equation to (73), we obtain (17), where

$$P(\Theta) = J_{Z1}^T N_1 J_\theta^T + J_{Z2}^T \tag{77}$$

$$Q(\Theta, \dot{\Theta}) = J_{Z1}^T N_2 \mathbf{C}_0 \tag{78}$$

$$R(\Theta, g, \mathbf{F}) = J_{Z1}^T N_1 \mathbf{G}_0. \tag{79}$$

8. References

Behnke, S. (2006). Online Trajectory Generation for Omnidirectional Biped Walking, *Proceedings of IEEE International Conference on Robotics and Automation (ICRAAf06), Orlando, Florida* pp. 1597–1603.

Czarnetzki, S., Kerner, S. & Urbann, O. (2009). Observer-based dynamic walking control for biped robots, *Robotics and Autonomous Systems* 57(8): 839–845.

Goswami, A. (1999). Postural Stability of Biped Robots and the Foot-Rotation Indicator (FRI) Point, *The International Journal of Robotics Research* 18(6): 523.

Héliot, R. & Espiau, B. (2008). Online generation of cyclic leg trajectories synchronized with sensor measurement, *Robotics and Autonomous Systems* 56(5): 410–421.

Hirai, K., Hirose, M., Haikawa, Y. & Takenaka, T. (1998). The development of Honda humanoid robot, *Robotics and Automation, 1998. Proceedings. 1998 IEEE International Conference on* 2.

Horak, F. & Nashner, L. (1986). Central programming of postural movements: adaptation to altered support-surface configurations, *Journal of Neurophysiology* 55(6): 1369–1381.

Huang, Q., Kaneko, K., Yokoi, K., Kajita, S., Kotoku, T., Koyachi, N., Arai, H., Imamura, N., Komoriya, K. & Tanie, K. (2000). Balance control of a biped robot combining off-line pattern with real-time modification, *Proc. of the 2000 IEEE International Conference on Robotics and Automation* 4: 3346–3352.

Ito, S., Asano, H. & Kawasaki, H. (2003). A balance control in biped double support phase based on center of pressure of ground reaction forces, *7th IFAC Symposium on Robot Control* pp. 205–210.

Ito, S. & Kawasaki, H. (2005). Regularity in an environment produces an internal torque pattern for biped balance control, *Biological Cybernetics* 92(4): 241–251.

Ito, S., Amano, S., Sasaki, M. & Kulvanit, P. (2007). In-place lateral stepping motion of biped robot adapting to slope change, *Proceedings of the 2007 IEEE International Conference on Systems, Man and Cybernetics* pp. 1274–1279.

Ito, S., Amano, S., Sasaki, M. & Kulvanit, P. (2008). A ZMP Feedback Control for Biped Balance and its Application to In-Place Lateral Stepping Motion, *JOURNAL OF COMPUTERS* 3(8): 23.

Kagami, S., Kitagawa, T., Nishiwaki, K., Sugihara, T., Inaba, M. & Inoue, H. (2002). A Fast Dynamically Equilibrated Walking Trajectory Generation Method of Humanoid Robot, *Autonomous Robots* 12(1): 71–82.

Kajita, S. & Tani, K. (1996). Experimental study of biped dynamic walking, *Control Systems Magazine, IEEE* 16(1): 13–19.

Kulvanit, P., Wongsuwan, H., Srisuwan, B., Siramee, K., Boonprakob, A., Maneewan, T. & Laowattana, D. (2005). Team KMUTT: Team Description Paper, *Robocup 2005: Humanoid League* .

Lee, B., Kim, Y. & Kim, J. (2005). Balance control of humanoid robot for hurosot, *Proc. of IFAC World Congress* .

McGhee, R. & Frank, A. (1968). On the stability properties of quadruped creeping gaits, *Mathematical Biosciences* 3(3-4): 331–351.

Mitobe, K., Capi, G. & Nasu, Y. (2001). Control of walking robots based on manipulation of the zero moment point, *Robotica* 18(06): 651–657.

Nagasaka, K., Inoue, H. & Inaba, M. (1999). Dynamic walking pattern generation for a humanoid robot based on optimal gradient method, *Proc. of 1999 IEEE International Conference on Systems, Man and Cybernetics* 6.

Napoleon, S. & Sampei, M. (2002). Balance control analysis of humanoid robot based on ZMP feedback control, *Proceedings of the 2002 IEEE/RSJ International Conference on Intelligent Robots and Systems* pp. 2437–2442.

Nishiwaki, K., Kagami, S., Kuniyoshi, Y., Inaba, M. & Inoue, H. (2002). Online generation of humanoid walking motion based on a fast generation method of motion pattern that follows desired ZMP, *IEEE/RSJ 2002 International Conference on Intelligent Robots and System* 3.

Prahlad, V., Dip, G. & Meng-Hwee, C. (2007). Disturbance rejection by online ZMP compensation, *Robotica* 26(1): 9–17.

Sugihara, T., Nakamura, Y. & Inoue, H. (2002). Real-time humanoid motion generation through ZMP manipulation based on inverted pendulum control, *Proceedings of 2002 IEEE International Conference on Robotics and Automation* 2.

Suleiman, W., Kanehiro, F., Miura, K. & Yoshida, E. (2009). Improving ZMP-based control model using system identification techniques, *9th IEEE-RAS International Conference on Humanoid Robots*, pp. 74–80.

Wollherr, D. & Buss, M. (2004). Posture modification for biped humanoid robots based on Jacobian method, *Proceedings. 2004 IEEE/RSJ International Conference on Intelligent Robots and Systems(IROS 2004)* 1.

Yamaguchi, J. & Takanishi, A. (1997). Development of a Leg Part of a Humanoid Robot?Development of a Biped Walking Robot Adapting to the Humans' Normal Living Floor, *Autonomous Robots* 4(4): 369–385.

Biped Robots

Edited by Prof. Armando Carlos Pina Filho

Biped robots represent a very interesting research subject, with several particularities and scope topics, such as: mechanical design, gait simulation, patterns generation, kinematics, dynamics, equilibrium, stability, kinds of control, adaptability, biomechanics, cybernetics, and rehabilitation technologies. We have diverse problems related to these topics, making the study of biped robots a very complex subject, and many times the results of researches are not totally satisfactory. However, with scientific and technological advances, based on theoretical and experimental works, many researchers have collaborated in the evolution of the biped robots design, looking for to develop autonomous systems, as well as to help in rehabilitation technologies of human beings. Thus, this book intends to present some works related to the study of biped robots, developed by researchers worldwide.

How to reference

In order to correctly reference this scholarly work, feel free to copy and paste the following:

INTECH
open science | open minds